Journal of Materials Chemistry A

RSC Publishing

PAPER

View Article Online
View Journal | View Issue

Published on 05 November 2012. Downloaded by National Chiao Tung University on 28/04/2014 02:09:41.

Cite this: *J. Mater. Chem. A*, 2013, **1**, 1310

Novel pyrene- and anthracene-based Schiff base derivatives as Cu^{2+} and Fe^{3+} fluorescence turn-on sensors and for aggregation induced emissions†

Muthaiah Shellaiah, Yen-Hsing Wu, Ashutosh Singh, Mandapati V. Ramakrishnam Raju and Hong-Cheu Lin*

Novel pyrene- and anthracene-based Schiff base derivatives **P1** and **A1** were synthesized *via* a one-pot reaction and utilized as fluorescence turn-on sensors towards Cu^{2+} and Fe^{3+} ions, respectively, and for aggregation induced emissions (AIEs). **P1** in CH_3CN and **A1** in THF illustrated the fluorescence turn-on sensing towards Cu^{2+} and Fe^{3+} ions, respectively, *via* chelation enhanced fluorescence (CHEF) through excimer (**P1–P1*** and **A1–A1***) formation. The 2 : 1 stoichiometry of the sensor complexes (**P1** + Cu^{2+} and **A1** + Fe^{3+}) were calculated from Job plots based on UV-Vis absorption titrations. In addition, the binding sites of sensor complexes (**P1** + Cu^{2+} and **A1** + Fe^{3+}) were well established from the ^1H NMR titrations and supported by the fluorescence reversibility by adding metal ions and **PMDTA** sequentially. The detection limits (LODs) and the association constant (K_a) values of **P1** + Cu^{2+} and **A1** + Fe^{3+} sensor responses were calculated by standard deviations, linear fittings and from their fluorescence binding isotherms. More importantly, **P1** + Cu^{2+} and **A1** + Fe^{3+} sensors were found to be active in wide ranges of pHs (1–14 and 2–14, respectively). Moreover, the time effect along with the enhancements of quantum yield (Φ) and time resolved photoluminescence (TRPL) decay constant (τ) towards sensor responses were investigated. Similarly, **P1** in CH_3CN and **A1** in THF showed AIEs by increasing the aqueous media concentration from 0% to 90%, with altered fluorescence peak shifts (red and blue shifts, respectively). As well as τ value enhancements, the Φ values of 0.506 and 0.567 (with 630- and 101-fold enhancements) were acquired for **P1** in CH_3CN : H_2O (20 : 80) and **A1** in THF : H_2O (40 : 60), respectively.

Received 5th October 2012
Accepted 2nd November 2012

DOI: 10.1039/c2ta00574c

www.rsc.org/MaterialsA

Introduction

Owing to the biological and environmental importance of metal ions, numerous sensory reports are available for different metal ions with diverse mechanisms.[1] Among the available detection methods, chemosensors based on ion-induced fluorescence changes are predominantly attractive in terms of sensitivity, selectivity, response time and local observation (*e.g.*, fluorescence imaging spectroscopy).[2] Due to the fluorescence quenching effects[3] of biologically important ions, the development of fluorescence turn-on sensors still remains a challenging task. Several molecular turn-on sensors[4] were reported for a variety of cations and anions based on photoinduced electron transfer (PET), internal charge transfer (ICT), chelation enhanced fluorescence (CHEF) and deprotonation mechanisms. Among them, PET[5] exhibited various changes of emission intensities with some or no spectral shifts, whereas ICT[6] caused both intensity changes and spectral shifts, and CHEF[7] also provided fluorescence enhancements with or without any spectral changes.

Among all metal ions, Cu^{2+} is a significant metal pollutant due to its widespread use,[8] but it is also required as a cofactor in nearly 20 enzymes[9] and is an essential micro-nutrient for all known life forms. Moreover, long-term exposure to high levels of Cu^{2+} has been reported to induce liver and kidney damage.[10] In addition, most of the copper-selective sensors suffer from the interfering effect[11] of cations, such as Zn^{2+}, Hg^{2+}, Pb^{2+}, Fe^{3+} and Ag^{+}. Therefore, the development of highly selective fluorescence probes[12] for copper ions in the presence of a variety of other metal ions has received great interest. Similarly, the Fe^{3+} ion is essential for the proper functioning of all living cells, but it is detrimental when present in excess.[13] Most of the iron present in biological systems is tightly associated with enzymes, as well as in specialized transport and storage in proteins.[14] Furthermore, iron homeostasis is an important factor involved in neuroinflammation and the progression of Alzheimer's disease.[15] Many sensor reports[16] are available for Cu^{2+} and Fe^{3+} ions along with synthetic difficulties, but only a few of them were accounted as turn-on sensors. Hence, we tend to develop the specific sensory materials for Cu^{2+} and Fe^{3+} detections with optical turn-on responses *via* simple synthetic pathways.

Department of Materials Science and Engineering, National Chiao Tung University, Hsinchu 30049, Taiwan (ROC). E-mail: linhc@mail.nctu.edu.tw

† Electronic supplementary information (ESI) available. See DOI: 10.1039/c2ta00574c

This journal is © The Royal Society of Chemistry 2013

Published on 05 November 2012. Downloaded by National Chiao Tung University on 28/04/2014 02:09:41.

Similar to sensor applications, aggregation induced emission (AIE) has become more popular and has also been applied to many areas of science[17] by Tang *et al.* during the last decade. Molecules with AIE characteristics have been found to serve as chemosensors, bioprobes, stimuli-responsive nanomaterials and active layers in the construction of efficient organic light-emitting diodes.[18] However, many of these molecules also have synthetic difficulties, so we try to develop molecules that could exhibit the AIE effects with less synthetic difficulties.

With these considerations, Schiff bases[19] are recognized as having simple synthetic steps and are also applied to many optical sensors, as well as in AIE applications. However, to develop Schiff bases with sensor and AIE properties, the presence of strong fluorophores are required.[20] Pyrene and anthracene derivatives were evidenced as excellent fluorophores and widely used in the developments of fluorescence (FL) sensors because of their excellent photoluminescence properties and chemical stabilities. Furthermore, pyrene and anthracene fluorescent probes self-assembled to form dimeric structures upon the addition of certain metal cations to give **P–P*** and **A–A*** excimer fluorescence and also provided the AIE characteristics by tuning the solvent conditions as reported previously.[21] Therefore, we developed the novel pyrene- and anthracene-based Schiff bases and evaluated their sensor and AIE properties (Fig. 1).

Herein, we report novel pyrene- and anthracene-based Schiff base derivatives (**P1** and **A1**) for the first time as Cu^{2+} and Fe^{3+} turn-on sensors *via* CHEF and excimer formations and these were also utilized for aggregation induced emissions (AIEs) by increasing the concentration of H_2O (0–90%) with huge quantum yield (Φ) enhancements.

Results and discussion

Synthesis

As shown in Scheme 1, **P1** and **A1** were synthesized *via* a one pot aldehyde and amine condensation in methanol with 98 and 71% yields, respectively.

Computational analysis

Computational analyses of **P1** and **A1** were carried out *via* the semi-empirical (AM1) method,[22] as evidenced in Fig. 2. It reveals the HOMO of **P1** positioned in the imine group and the LUMO in the pyrene ring. Similarly, the HOMO electron clouds of **A1** were located in the imine group and the LUMO electron clouds were in both phenyl and anthracene rings.

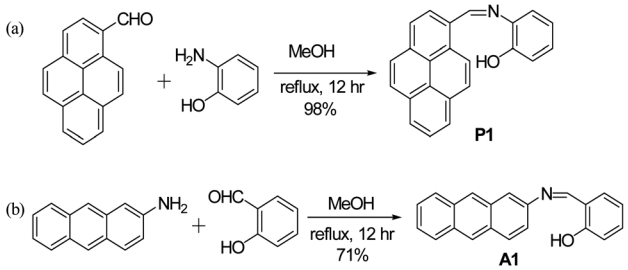

Scheme 1 Synthesis of **P1** and **A1**.

Photophysical properties of Schiff bases and sensor complexes

The photophysical properties of **P1** and **A1** and sensor complexes (**P1** + Cu^{2+} and **A1** + Fe^{3+}) are shown in Table 1. Both Schiff bases **P1** and **A1** were excited at 395 nm and showed PL emission maxima at 459 and 499 nm, respectively. Since excess additions of water to **P1** in CH_3CN and **A1** in THF caused the aggregation induced emissions, we performed UV-Vis/PL sensor titrations of **P1** and **A1** in CH_3CN and THF, respectively, by adding metal ions in pure H_2O. Similarly, ^1H titrations were performed in CD_3CN and [D_8]-THF, respectively, by adding metal ions in D_2O. The quantum yield (Φ) enhancements of the sensor complexes (**P1** + Cu^{2+} and **A1** + Fe^{3+}) were observed as shown in Table 1. In general, sensor devices based on organic semiconducting materials should not be dissolved in water and also should possess p- or n-type semi-conducting properties. Moreover, those materials must have some probes that can provide the selectivities towards the specific analytes in organic solvents.[23] Since pyrene and anthracene derivatives have the p-type semiconducting properties, the utilization of **P1** and **A1** as metal ion sensors in organic solvents and their insolubilities in water were considered as advantages for sensor devices in the near future. At the same time, to discriminate the sensory and AIE properties of **P1** and **A1**, all the metal ions were taken from 1 mM concentration rather than 1×10^{-4} M and hence the

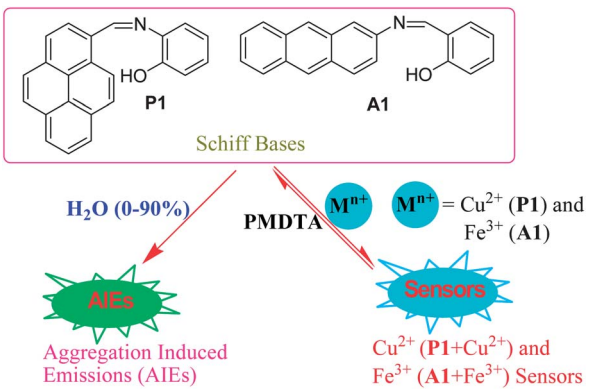

Fig. 1 Schematic representations of sensors and aggregation induced emissions (AIEs) of Schiff bases.

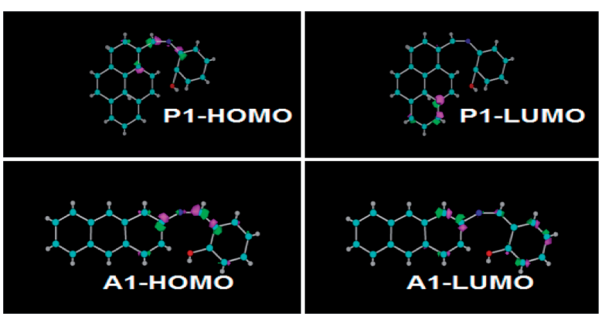

Fig. 2 Computational analysis of HOMO and LUMO levels of **P1** and **A1** (semi-empirical AM1 method).

Published on 05 November 2012. Downloaded by National Chiao Tung University on 28/04/2014 02:09:41.

Table 1 Photophysical properties of Schiff bases and sensor complexes

Compounds	CHEF[a]	Association constant[b] (K_a)	Detection limits (LODs)[c]	Quantum yield[d] (Φ)	Quantum yield (Φ) enhancements	τ[e] (ns)
P1 (λ_{ex} = 395 and λ_{em} = 459 nm)	NA	NA	NA	0.0009	NA	1.30
A1 (λ_{ex} = 395 and λ_{em} = 499 nm)	NA	NA	NA	0.005	NA	10.60
P1 + Cu^{2+} (λ_{ex} = 395 and λ_{em} = 455 nm)	591 fold	1.96×10^6 M^{-1}	9.72×10^{-7} M	0.284	315 fold	2.05
A1 + Fe^{3+} (λ_{ex} = 395 and λ_{em} = 495 nm)	35 fold	1.88×10^5 M^{-1}	2.95×10^{-6} M	0.125	25 fold	12.46

[a] I/I_0 values were reported as Chelation enhanced fluorescence (CHEF). [b] Association constants were calculated from the slopes of binding isotherms. [c] Detection limits (LODs) were obtained from their fluorescence binding isotherms. [d] Quantum yields were calculated using 9,10-diphenylanthracene (Φ = 0.9) as a reference standard. [e] Obtained from time resolved fluorescence measurements.

differences between sensory and AIEs of **P1** and **A1** were well established.

Fluorescence titrations on metal ions

Initially, **P1** (20 μM) in CH_3CN and **A1** (20 μM) in THF were investigated towards 60 μM (3 equiv.) of metal ions (Li^+, Ag^+, K^+, Na^+, Cs^+, Ni^{2+}, Fe^{3+}, Co^{2+}, Zn^{2+}, Cd^{2+}, Pb^{2+}, Ca^{2+}, Cr^{3+}, Mg^{2+}, Cu^{2+}, Mn^{2+}, Hg^{2+}, Fe^{2+} and Ag^{2+}) in H_2O. As noticed in Fig. 3, **P1** and **A1** show better selectivities to Cu^{2+} and Fe^{3+} ions, respectively, upon treatment with 2.5 and 3 equiv. of metal ions, respectively. Furthermore, the CHEF for **P1** + Cu^{2+} and **A1** + Fe^{3+} were found to be 591 and 35 fold, respectively and with 315 fold (**P1** + Cu^{2+}; Φ = 0.284) and 25 fold (**A1** + Fe^{3+}; Φ = 0.125) of quantum yield enhancements. In addition, the above selectivities were confirmed further by single and dual metal studies as follows. In order to establish the specific selectivities of **P1** and **A1** to Cu^{2+} and Fe^{3+}, respectively, we performed the single and dual metal competitive analysis, as shown in Fig. 4. In a single metal system (black bars), all the metal (Li^+, Ag^+, K^+, Na^+, Cs^+, Ni^{2+}, Fe^{3+}, Co^{2+}, Zn^{2+}, Cd^{2+}, Pb^{2+}, Ca^{2+}, Cr^{3+}, Mg^{2+}, Cu^{2+}, Mn^{2+}, Hg^{2+}, Fe^{2+} and Ag^{2+} in H_2O) concentrations were kept as 50 μM towards **P1**. However, for the dual-metal (white bars) studies, two equal amounts of aqueous solutions of Cu^{2+} and other metal ions (50 μM + 50 μM) were combined. During the single metal analysis, the Cu^{2+} effect at 100 μM was taken. Similarly, those metal ions concentrations were kept as 60 μM towards **A1** in the single metal system (black bars) and for dual-metal (white bars) studies, two equal amounts of aqueous solutions of Fe^{3+} and other metal ions (60 μM + 60 μM) were combined. Furthermore, in the single metal analysis, the Fe^{3+} effect at 120 μM was investigated. In addition to the selectivity of **A1** towards Fe^{3+} ions, Fe^{2+} ions also showed little selectivity (Fig. 3) with 15 fold of CHEF and 7 fold quantum yield enhancements. However, further sensing enhancements of **A1** towards Fe^{2+} in CHEF and Φ values w.r.t ratiometric titrations (0–5 equiv.) was not evidenced, so the better selectivity of **A1** to Fe^{3+} ions was confirmed. Moreover, the specific selectivities of **P1** and **A1** by single and dual metal studies also confirmed their respective selectivities towards Cu^{2+} and Fe^{3+} ions, as shown in Fig. 4. The photographs of **P1** + Cu^{2+} and **A1** + Fe^{3+} (under UV-light irradiations) well demonstrated their sensitivities by strong blue and green fluorescences, respectively, as depicted in Fig. 5a and b. On the other hand, modest selectivity of **A1** to Cu^{2+} and Fe^{2+} was also visualized by the photograph shown in Fig. 5c.

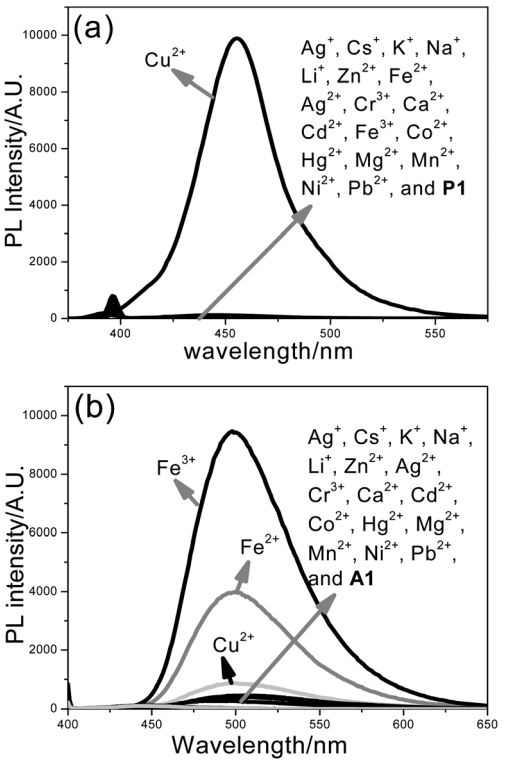

Fig. 3 Sensor responses of (a) **P1** (1×10^{-5} M) in CH_3CN (λ_{ex} = 395 nm) and (b) **A1** (1×10^{-5} M) in THF (λ_{ex} = 395 nm) towards metal ions (note: each metal selectivity was measured with 2.5 and 3 equiv. of metal ions, respectively).

Fluorescence titrations on Cu^{2+} and Fe^{3+} sensors

By increasing the concentrations of Cu^{2+} (0–50 μM with an equal span of 2 μM in H_2O) the sensitivity of **P1** (20 μM) in CH_3CN towards Cu^{2+} ions was clearly observed in Fig. 6a. The fluorescence spectrum of **P1** (λ_{em} = 455 nm) showed the rapid turn-on responses and the inset illustrated the relative fluorescence intensity changes as a function of Cu^{2+} concentration. On the other hand, upon the addition of Fe^{3+} (0–60 μM with an equal span of 2 μM in H_2O) the sensitivity of **A1** (20 μM) in THF towards Fe^{3+} ions was evidenced in Fig. 6b. The fluorescence spectrum of **A1** (λ_{em} = 495 nm) exhibited turn-on responses

 This journal is © The Royal Society of Chemistry 2013

Published on 05 November 2012. Downloaded by National Chiao Tung University on 28/04/2014 02:09:41.

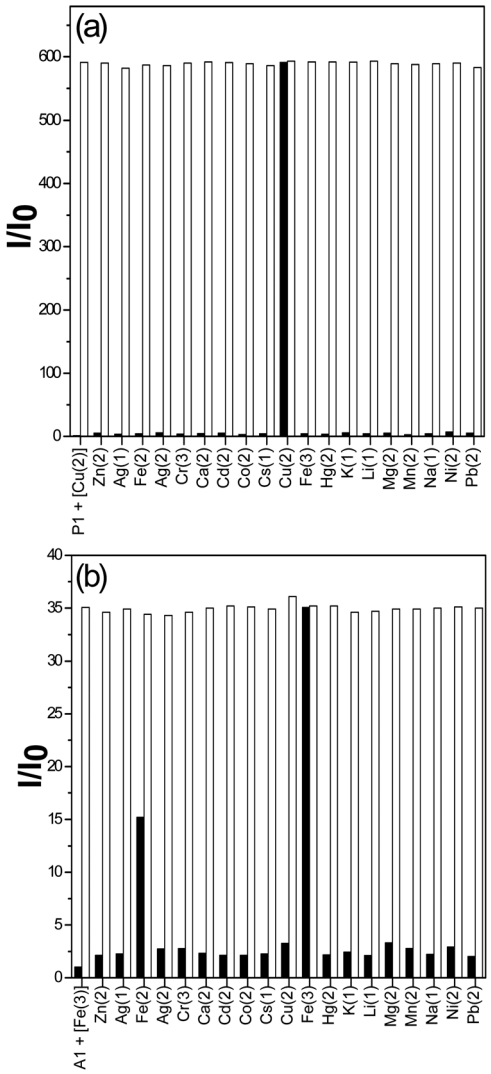

Fig. 4 Relative fluorescence intensities of (a) **P1** (20 μM) in CH_3CN (λ_{ex} = 395 nm) with 50 μM of Cu^{2+} in H_2O and (b) **A1** (20 μM) in THF (λ_{ex} = 395 nm) with 60 μM Fe^{3+} in H_2O in the presence of competing metal ions. Black bar; **P1** (20 μM) in CH_3CN and **A1** (20 μM) in THF with 50 and 60 μM of stated metal ions in H_2O, respectively. White bar; **P1** (20 μM) in CH_3CN with 50 μM Cu^{2+} + 50 μM of stated metal ions and **A1** (20 μM) in THF with 60 μM Fe^{3+} + 60 μM of stated metal ions in H_2O. (100 and 120 μM of Cu^{2+} and Fe^{3+} were taken for Cu^{2+} and Fe^{3+} effects, respectively).

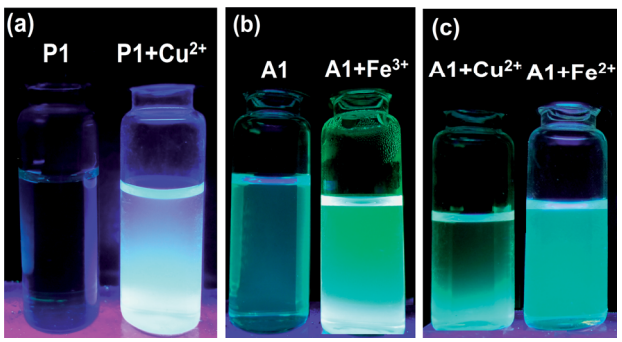

Fig. 5 Photographs of (a) **P1**, **P1** + Cu^{2+}, (b) **A1**, **A1** + Fe^{3+} and (c) **A1** + Cu^{2+}, **A1** + Fe^{2+} visualized under UV-light irradiations (λ = 365 nm).

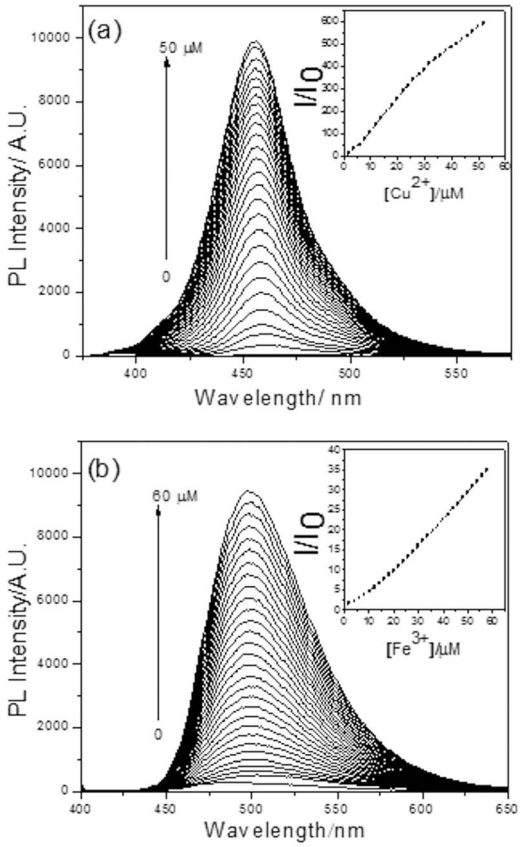

Fig. 6 Fluorescence spectra of (a) **P1** (20 μM) in CH_3CN (λ_{ex} = 395 nm) with 0–50 μM of Cu^{2+} in H_2O (with an equal span of 2 μM) and (b) **A1** (20 μM) in THF (λ_{ex} = 395 nm) with 0–60 μM of Fe^{3+} in H_2O (with an equal span of 2 μM); insets: relative fluorescence intensity changes with respect to Cu^{2+} and Fe^{3+} concentrations.

rapidly and the inset demonstrated the relative fluorescence intensity changes as a function of Fe^{3+} concentration. Furthermore, the CHEF values of **P1** + Cu^{2+} and **A1** + Fe^{3+} sensor responses increased 591 and 35 folds, respectively, due to their strong fluorescence natures. Similarly, the quantum yield (Φ) values of **P1** + Cu^{2+} and **A1** + Fe^{3+} also increased 315 and 25 fold, respectively, as shown in Table 1.

Stoichiometries[24] and binding sites

To ensure the binding sites of sensor responses of **P1** and **A1**, the stoichiometries of **P1** + Cu^{2+} and **A1** + Fe^{3+} were calculated through Job's plots as shown in Fig. S7 and S8 (ESI†) the stoichiometries of **P1** + Cu^{2+} and **A1** + Fe^{3+} were established by Job's plots between the mole fraction (X_M) and absorption maximum changes at 395 and 346 nm, respectively. Upon the addition of 0–30 μM of Cu^{2+} or Fe^{3+} (with an equal span of 3 μM), the absorption maxima of **P1** and **A1** were quenched rapidly up to 10 μM, afterwards they were found to be restored again. Therefore, the Job's plots were plotted between X_M and absorption changes at 395 nm (**P1** + Cu^{2+}) and 346 nm (**A1** + Fe^{3+}), where they went through maxima at molar fractions of *ca.* 0.412 (**P1** + Cu^{2+}) and 0.370 (**A1** + Fe^{3+}), respectively, as shown in Fig. S7b and S8b (ESI†), representing their 2 : 1 stoichiometric complexes. As shown in Fig. 7, the stoichiometries were further

Published on 05 November 2012. Downloaded by National Chiao Tung University on 28/04/2014 02:09:41.

supported by ^{1}H NMR titrations[25] along with binding sites confirmation. In addition to stoichiometry, the total disappearance of the –OH peaks upon the addition of 0.5 equiv. of metal ions (Cu^{2+} and Fe^{3+} ions) confirmed the involvement of hetero atoms (O and N) and their chelation to form the excimers (**P1–P1*** and **A1–A1***) in the sensing mechanism. Moreover, the binding site and the excimers mechanism were well supported by the reversibilities of **P1** + Cu^{2+} and **A1** + Fe^{3+} sensor complexes. Both sensors (**P1** + Cu^{2+} and **A1** + Fe^{3+}) were found to be reversible to their original state upon the addition of 2 drops of 50% pentamethyl diethylene triamine (PMDTA)[26] in CH_3CN or THF and can be reused for up to 4 cycles as established in Fig. S10 (ESI†). Therefore, the possible sensing mechanism based on the excimer formation was proposed as noted in Fig. 8.

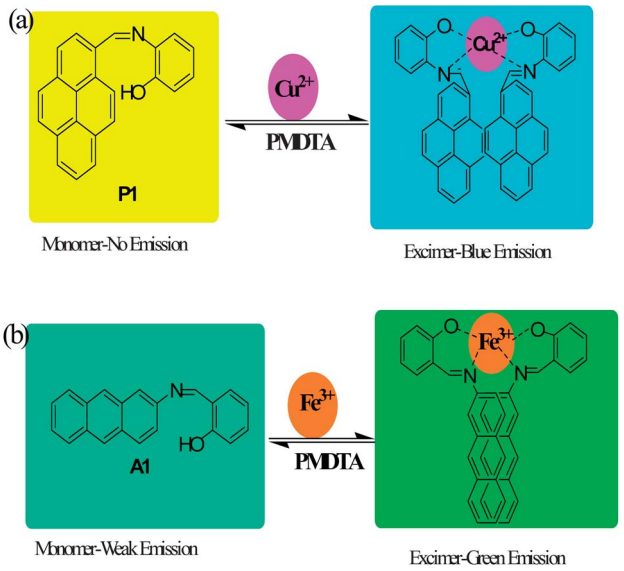

Fig. 8 Possible proposed binding mechanism of (a) **P1** and (b) **A1**, towards Cu^{2+} and Fe^{3+} ions.

Detection limits (LODs) and association constants (K_a)

In order to prove the selectivities of **P1** and **A1** towards Cu^{2+} and Fe^{3+}, respectively, the calculations of detection limits (LODs)[27] were performed through standard deviations and linear fittings as shown in Fig. S9 (ESI†). By plotting the relative fluorescence intensity (I/I_0) changes as a function of concentration the detection limits of **P1** + Cu^{2+} and **A1** + Fe^{3+} were calculated as 9.72×10^{-7} and 2.95×10^{-6} M, respectively. Assuming a 2 : 1 complex formation, the association constant (K_a) was calculated on the basis of the titration curves of the sensor **P1** and **A1** with Cu^{2+} and Fe^{3+}. As shown in Fig. S13 (ESI†), the association constants[28] were determined by a linear least square fitting of data with $[Cu^{2+}] = 1/2K_a[L]_T.\ x/(1-x^2) + [L]_T/2.\ x$ and $[Fe^{3+}] = 1/3K_a[L]_T.\ x/(1-x^3) + [L]_T/3.\ x$ equations, respectively. Where K_a is the complex association constant; $[Cu^{2+}]$ and $[Fe^{3+}]$ are the concentrations of Cu^{2+} and Fe^{2+} ions; $[L]_T$ is the initial concentration of the sample; $x = I - I_0/I_{max} - I_0$; I, I_0 and I is the absorption intensity at 455 nm (**P1**) or 495 nm (**A1**) of the respective species, free ligand and the absorption intensity at 455 nm (**P1**) or 495 nm (**A1**) upon the addition of Cu^{2+} and Fe^{3+}, respectively. The K_a values of **P1** + Cu^{2+} and **A1** + Fe^{3+} were estimated as 1.96×10^6 and 1.88×10^5 M^{-1}, respectively. Furthermore, to confirm the better selectivities of **P1** and **A1** towards Cu^{2+} and Fe^{3+}, respectively, the pH and time effects of their sensor responses are evaluated as explained below.

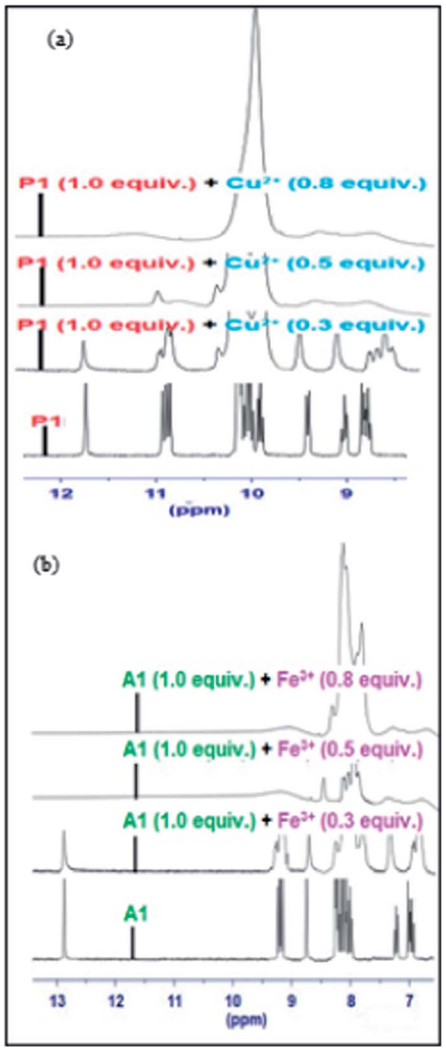

Fig. 7 NMR spectral changes of (a) **P1** (20 mM) in d-acetonitrile and (b) **A1** (20 mM) in d-tetrahydrofuran titrated with 0–16 mM of Cu^{2+} and Fe^{3+} in D_2O.

pH and time effects[29]

The **P1** + Cu^{2+} and **A1** + Fe^{3+} sensor responses were verified between pH 0 and 14, maintained by the respective buffers (100 μM). In contrast to separate titrations (Fig. S12, ESI†) of pHs (0–14) solutions (100 μM) to **P1** and **A1**, the **P1** + Cu^{2+} and **A1** + Fe^{3+} sensors were active in wide ranges of pHs (1–14 and 2–14, respectively) in both cases, as shown in Fig. S11 (ESI†). The above observation confirmed that **P1** and **A1** can also be utilized as pH sensors to distinguish acidic and basic pHs. Assuming a 2 : 1 complex formation, the time-dependent fluorescent analyses of **P1** (20 μM) in CH_3CN and **A1** (20 μM) in THF were carried out by adding 10 μM (0.5 equiv.) of metal ions in H_2O, as shown

 This journal is © The Royal Society of Chemistry 2013

Published on 05 November 2012. Downloaded by National Chiao Tung University on 28/04/2014 02:09:41.

in Fig. S14 (ESI†). Both **P1** + Cu^{2+} and **A1** + Fe^{3+} sensor responses in time dependent analyses demonstrated identical results as shown in Fig. 6. As noticed in Fig. S14c and d,† the relative fluorescence intensity changes also reached the maximum CHEF values after 10 minutes. The time resolved photoluminescence (TRPL) measurements were proceeded further to reconfirm the turn-on sensor responses of **P1** and **A1** towards Cu^{2+} and Fe^{3+} ions, respectively.

Counter ion effect on sensor responses[30]

Since many sensor responses are affected by the presence of counter ions, we performed the sensor titrations of **P1** and **A1** towards Cu^{2+} and Fe^{3+}, respectively, with different counterion salts. As evidenced in Fig. S15a (ESI†), the Cu^{2+} sensor response was found to be increased from 591 fold to 620 fold in the presence of hydroxide (OH^-) as a counter ion. However, the sensor response in the presence of acetate (CH_3COO^-) provided just 553 fold CHEF enhancement. In the same way, the CHEF values of Cu^{2+} sensor responses of other counter ions (NO_3^-, Cl^-, Br^-, ClO_4^-, IO_3^- and SO_4^{2-}) lies between 560 and 591 fold. Similar to the Cu^{2+} sensor response of **P1**, the **A1** sensor response towards Fe^{3+} (Fig. S15b, ESI†) also indicated the CHEF value increased from 35 to 42 fold in the presence of hydroxide (OH^-) as a counter ion. However, the presence of other counter ions (CN^-, NO_3^-, Cl^-, F^-, ClO_4^-, IO_3^- and SO_4^{2-}) produced the CHEF values between 30 and 35 fold. Hence, it was concluded that both the Cu^{2+} and Fe^{3+} sensor responses of **P1** and **A1** were not affected incredibly in the presence of different counter ions.

Time resolved photoluminescence spectra (TRPL)[31]

As reported in the literature and from our results (Fig. 9a and b), we found that the fluorescence decay constants (τ) were affected typically by turn-on sensor responses as summarized in Tables 1 and S1 (ESI†). From the TRPL signals without any sensor responses the fluorescence life time values of **P1** and **A1** were 1.30 and 10.60 ns, respectively. During the **P1** + Cu^{2+} and **A1** + Fe^{3+} sensing processes, the faster decay components (A_1) of **P1** and **A1** (35.58% and 14.31%) were increased to 96.16% and 23.51%, respectively, along with decreased values of longer decay components (A_2), as shown in Table S1 (ESI†). Based on single exponential decay fittings, the average fluorescence life time values of **P1** + Cu^{2+} and **A1** + Fe^{3+} were estimated as 2.05, and 12.46 ns, respectively. The increased decay constant (τ) values of **P1** + Cu^{2+} and **A1** + Fe^{3+} verified the turn-on sensor responses of **P1** and **A1** through CHEF and excimer formations.

Aggregation induced emissions (AIEs) by Schiff bases

More interestingly, while preparing the stock solutions of **P1** in CH_3CN and **A1** in THF by varying the water concentrations for sensor titrations, the fluorescence spectra of **P1** and **A1** were enhanced with spectral shifts w.r.t time (0–18 hours) due to their aggregated nature. Hence, we proceeded the aggregation induced emission (AIE) analysis further. As shown in Fig. 10, the PL intensities were enhanced by increasing the concentrations of H_2O (up to 90%), the PL emissions of **P1** (in CH_3CN) and **A1** (in THF) were shifted from 455 and 499 nm to 471 and 495 nm,

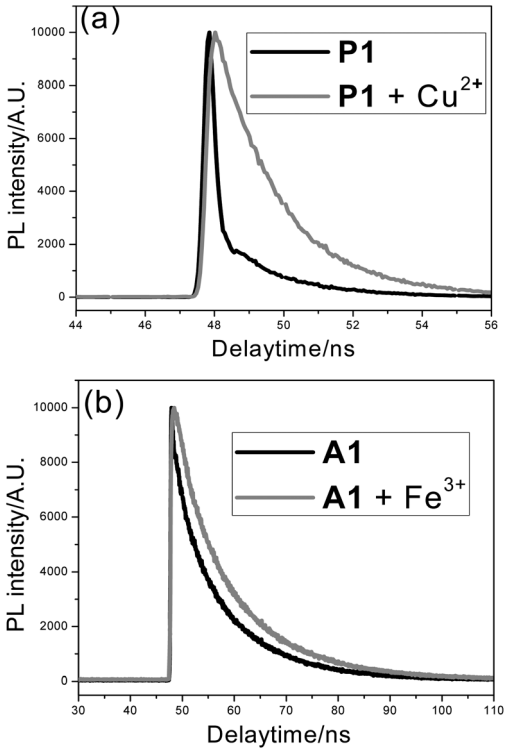

Fig. 9 Time resolved fluorescence spectra of (a) **P1** (black) and **P1** + Cu^{2+} (gray); (b) **A1** (black) and **A1** + Fe^{3+} (gray).

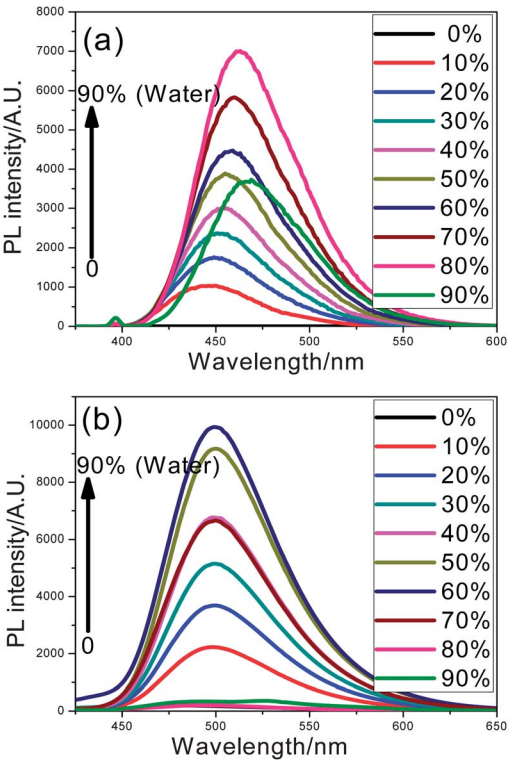

Fig. 10 Fluorescence spectra of (a) **P1** (2 μM) in CH_3CN (b) **A1** (2 μM) in THF, upon increasing the concentration of water from 0% to 90%. (Note: the spectra were taken after 18 hours).

Published on 05 November 2012. Downloaded by National Chiao Tung University on 28/04/2014 02:09:41.

respectively, in both extremes. Furthermore, as noticed in Table 2, the Φ values of 0.567 and 0.506 for **P1** in $CH_3CN : H_2O$ (20 : 80) and **A1** in THF : H_2O (40 : 60) were acquired with 630 and 101 fold enhancements, respectively. Upon increasing the concentration of H_2O (0–90%) in **P1** (in CH_3CN) and **A1** (in THF), the absorbance spectra (Fig. S16, ESI†) and the quantum yields (Fig. 11 and S17 (ESI†)) changes without certain trends w.r.t. time (0–18 hours), which also well proved the AIE characteristics of **P1** and **A1**. The fluorescence changes arose from AIE were visualized by the photographs (Fig. 11 (insets)) of **P1** (0 and 80%) and **A1** (0 and 60%). In addition, the TRPL spectra (Fig. S18, ESI†) and decay constant (τ) values (Tables 2 and S1 (ESI†)) of **P1** in $CH_3CN : H_2O$ (20 : 80) and **A1** in THF : H_2O (40 : 60) also confirmed their AIE nature. For **P1** in $CH_3CN : H_2O$ (20 : 80) and **A1** in THF : H_2O (40 : 60), the faster decay components (A_1) of **P1** and **A1** (35.58% and 14.31%) were increased and decreased to 71.31% and 8.40%, respectively, along with decreased and increased values of longer decay components (A_2) as shown in Table S1 (ESI†). As shown in Table 2, the single exponential fitting decay constant (τ) values of 4.13 and 22.30 ns for **P1** in $CH_3CN : H_2O$ (20 : 80) and **A1** in THF : H_2O (40 : 60) were both increased in contrast to 1.30 and 10.60 ns for **P1** (in CH_3CN) and **A1** (in THF), respectively.

Mechanism of AIEs by Schiff bases

As reported by previous literature,[32] the AIEs mechanism of both **P1** and **A1** possibly arose from the restriction of intramolecular rotation (RIR). Since, the single bond rotation is mainly responsible for the dominant nonradiative decay, the RIR effect might be the cause for the AIE nature of **P1** and **A1**. The hydrogen-bonded formation, suppression of PET process and suppression of charge transfer (CT) or intramolecular charge transfer (ICT) are the other mechanistic approaches for AIEs of **P1** and **A1**. However, our observations on the PL spectra of AIEs for **P1** and **A1** suggested that both the red and blue shifts by aggregation were probably originated from the suppression of twisted intramolecular charge transfer (TICT). The above justification was also well supported by the similar reports[33] available in the field of AIEs. As evidenced in Fig. 10 and 11, the PL spectra and Φ values of **P1** (in CH_3CN) and **A1** (in THF) were increased rapidly up to 80% and 60% of the water content arose from the suppressions of TICT processes. However, the PL spectra and Φ values of **P1** in $CH_3CN : H_2O$ (10 : 90) and **A1** in THF : H_2O (30 : 70 to 10 : 90) were found to be decreased due to the solvent effect on AIEs.[33]

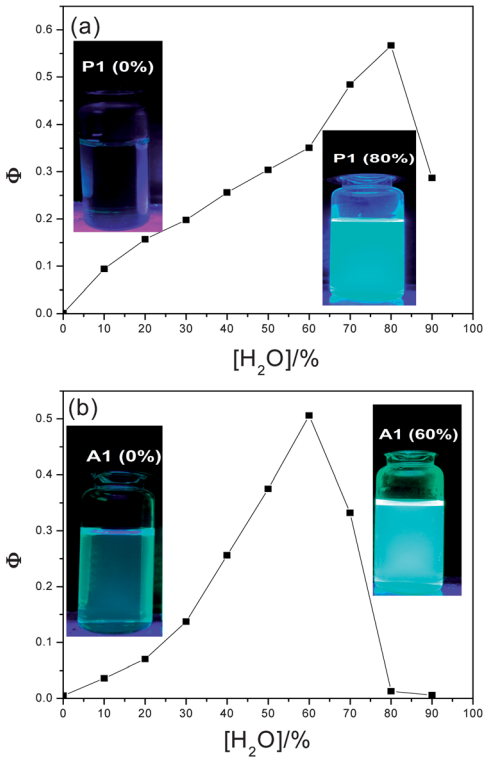

Fig. 11 Quantum yield (Φ) changes of (a) **P1** and (b) **A1**, upon increasing the concentration of water (0–90%), measured after 18 hours (note: quantum yield (Φ) calculations were carried out based on UV-Vis and PL spectral changes); insets: photographs of (a) **P1** in CH_3CN with 0% and 80% water and (b) **A1** in THF with 0% and 60% of water, visualized after 18 hours.

Table 2 Quantum yields (Φ) and TRPL decay constants (τ) values of **P1** (0% water), **A1** (0% water), **P1** (80% water) and **A1** (60% water)

Compounds	Quantum yield[a] (Φ)	Quantum yield (Φ) enhancements	τ^b (ns)
P1 (0%)	0.0009	NA	1.30
A1 (0%)	0.005	NA	10.60
P1 (80%)	0.567	630 folds	4.13
A1 (60%)	0.506	101 folds	22.30

[a] Quantum yields were calculated using 9,10-diphenylanthracene (Φ = 0.9) as a reference standard. [b] Obtained from time resolved fluorescence measurements.

Conclusions

In conclusion, novel pyrene- and anthracene-based Schiff base derivatives **P1** and **A1** were synthesized *via* a one-pot reaction and utilized as Cu^{2+} and Fe^{3+} turn-on sensors, respectively, and their preliminary AIE characteristics *via* increasing the concentration of H_2O (0–90%) were also established. The 2 : 1 stoichiometry of sensor complexes **P1** + Cu^{2+} and **A1** + Fe^{3+} were calculated from Job plots based on UV-Vis absorption titrations. In addition, the binding sites of sensor complexes **P1** + Cu^{2+} and **A1** + Fe^{3+} were well established from ^{1}H NMR titrations and supported by the fluorescence reversibility by adding metal ions and **PMDTA** sequentially. Hence, the possible sensing mechanisms through excimer formations were proposed. Furthermore, by standard deviations and linear fittings the detection limits (LODs) of **P1** + Cu^{2+} and **A1** + Fe^{3+} were calculated as 9.72×10^{-7} and 2.95×10^{-6} M, respectively. Similarly, based on fluorescent binding isotherms the association constant (K_a) values of **P1** + Cu^{2+} and **A1** + Fe^{3+} were estimated as 1.96×10^6 and 1.88×10^5 M^{-1}, respectively. More importantly, **P1** + Cu^{2+} and **A1** + Fe^{3+} sensors were found to be active in wide ranges of pHs (1–14 and 2–14, respectively) and also effective w.r.t time (0–10 minutes). Similar to the sensor properties, **P1** in

 This journal is © The Royal Society of Chemistry 2013

Published on 05 November 2012. Downloaded by National Chiao Tung University on 28/04/2014 02:09:41.

CH_3CN : H_2O (20 : 80) and **A1** in THF : H_2O (40 : 60) showed greater AIE properties with shifted PL emission peaks. In both applications, the huge enhancements of quantum yield (Φ) values were conceived in the analyses of the sensor (increased 315 and 25 folds) and AIE (increased 630 and 101 folds) measurements. Moreover, the sensor and AIE properties of **P1** and **A1** were also well supported by their TRPL spectra and decay constant (τ) values.

Acknowledgements

The financial supports of this project provided by the National Science Council of Taiwan (ROC) through NSC 99-2113-M-009-006-MY2 and NSC 99-2221-E-009-008-MY2 are acknowledged.

Notes and references

1 (*a*) V. Amendola, L. Fabbrizzi, F. Forti, M. Licchelli, C. Mangano, P. Pallavicini, A. Poggi, D. Sacchi and A. Taglieti, *Coord. Chem. Rev.*, 2006, **250**, 273; (*b*) D. Astruc, E. Boisselier and C. Ornelas, *Chem. Rev.*, 2010, **110**, 1857; (*c*) J. Wu, W. Liu, J. Ge, H. Zhang and P. Wang, *Chem. Soc. Rev.*, 2011, **40**, 3483.

2 (*a*) A. P. de Silva, H. Q. N. Gunaratne, T. Gunnlaugsson, A. J. M. Huxley, C. P. McCoy, J. T. Rademacher and T. E. Rice, *Chem. Rev.*, 1997, **97**, 1515; (*b*) A. K. Dwivedi, G. Saikia and P. K. Iyer, *J. Mater. Chem.*, 2011, **21**, 2502; (*c*) S. Sumalekshmy and C. J. Fahrni, *Chem. Mater.*, 2011, **23**, 483.

3 (*a*) N. Niamnont, R. Mungkarndee, I. Techakriengkrai, P. Rashatasakhon and M. Sukwattanasinitt, *Biosens. Bioelectron.*, 2010, **26**, 863; (*b*) X. Lou, D. Ou, Q. Li and Z. Li, *Chem. Commun.*, 2012, **48**, 8462.

4 (*a*) D. T. McQuade, A. E. Pullen and T. M. Swager, *Chem. Rev.*, 2000, **100**, 2537; (*b*) G. Aragay, J. Pons and A. Merkoci, *Chem. Rev.*, 2011, **111**, 3433.

5 M. Sauer, *Angew. Chem., Int. Ed.*, 2003, **42**, 1790.

6 (*a*) K. Hanaoka, Y. Muramatsu, Y. Urano, T. Terai and T. Nagano, *Chem.–Eur. J.*, 2010, **16**, 568; (*b*) Y. Chen, C. Zhu, Z. Yang, J. Li, Y. Chiao, W. He, J. Chen and Z. Guo, *Chem. Commun.*, 2012, **48**, 5094; (*c*) J. Wu, W. Liu, J. Ge, H. Zhang and P. Wang, *Chem. Soc. Rev.*, 2011, **40**, 3483.

7 (*a*) D. A. Pearce, N. Jotterand, I. S. Carrico and B. Imperiali, *J. Am. Chem. Soc.*, 2001, **123**, 5160; (*b*) M. Mameli, M. C. Aragoni, M. Arca, C. Caltagirone, F. Demartin, G. Farruggia, G. D. Filippo, F. A. Devillanova, A. Garau, F. Isaia, V. Lippolis, S. Murgia, L. Prodi, A. Pintus and N. Zaccheroni, *Chem.–Eur. J.*, 2010, **16**, 919; (*c*) Y. Bao, B. Liu, H. Wang, F. Du and R. Bai, *Anal. Methods*, 2011, **3**, 1274; (*d*) Y. Bao, B. Liu, F. Du, J. Tian, H. Wang and R. Bai, *J. Mater. Chem.*, 2012, **22**, 5291.

8 (*a*) M. F. Yardim, T. Budinova, E. Ekinci, N. Petrov, M. Razvigorova and V. Minkova, *Chemosphere*, 2003, **52**, 835; (*b*) M. Royzen, Z. Dai and J. W. Canary, *J. Am. Chem. Soc.*, 2005, **127**, 1612.

9 (*a*) R. L. Lieberman and A. C. Rosenzweig, *Nature*, 2005, **434**, 177; (*b*) K. Piontek, M. Antorini and T. Choinowski, *J. Biol. Chem.*, 2002, **277**, 37663; (*c*) K. C. Ko, J. S. Wu, H. J. Kim, P. S. Kwon, J. W. Kim, R. A. Bartsch, J. Y. Lee and J. S. Kim, *Chem. Commun.*, 2011, **47**, 3165.

10 E. L. Que, D. W. Domaille and C. J. Chang, *Chem. Rev.*, 2008, **108**, 1517.

11 R. G. Mohammad, P. Tahereh, H. B. Leila, R. Shohre, Y. Mohammad, R. K. Maryam, M. Abolghasem, A. Hossein and S. Mojtaba, *Anal. Chim. Acta*, 2001, **440**, 81.

12 (*a*) R. Martinez-Manez and F. Sancenon, *Chem. Rev.*, 2003, **103**, 4419; (*b*) L. Zheng, E. W. Miller, A. Pralle, E. Y. Esacoff and C. J. Chang, *J. Am. Chem. Soc.*, 2006, **128**, 10.

13 S. K. Sahoo, D. Sharma, R. K. Bera, G. Crisponi and J. F. Callan, *Chem. Soc. Rev.*, 2012, **41**, 7195, DOI: 10.1039/c2cs35152h.

14 (*a*) Y. Lu, S. M. Berry and T. D. Pfister, *Chem. Rev.*, 2001, **101**, 3047; (*b*) C. N. Roy and N. C. Andrews, *Hum. Mol. Genet.*, 2001, **10**, 2181.

15 E. C. Theil and D. J. Goss, *Chem. Rev.*, 2009, **109**, 4568.

16 (*a*) R. Sheng, P. Wang, Y. Gao, Y. Wu, W. Liu, J. Ma, H. Li and S. Wu, *Org. Lett.*, 2008, **10**, 5015; (*b*) S. Sirilaksanapong, M. Sukwattanasinitt and P. Rashatasakhon, *Chem. Commun.*, 2012, **48**, 293; (*c*) J. Du, M. Hu, J. Fan and X. Peng, *Chem. Soc. Rev.*, 2012, **41**, 4511; (*d*) Y. Xiang and A. Tong, *Org. Lett.*, 2006, **8**, 1549.

17 Y. Hong, J. W. Y. Lam and B. Z. Tang, *Chem. Soc. Rev.*, 2011, **40**, 5361.

18 (*a*) M. Wang, G. Zhang, D. Zhang, D. Zhu and B. Z. Tang, *J. Mater. Chem.*, 2010, **20**, 1858; (*b*) Z. Liu, W. Xue, Z. Cai, G. Zhang and D. Zhang, *J. Mater. Chem.*, 2011, **21**, 14487.

19 (*a*) V. Bhalla, R. Tejpal, R. Kumar and A. Sethi, *Inorg. Chem.*, 2009, **48**, 11677; (*b*) D. Maity, A. K. Manna, D. Karthigeyan, T. K. Kundu, S. K. Pati and T. Govindaraju, *Chem.–Eur. J.*, 2011, **17**, 11152; (*c*) S. Sumalekshmy and C. J. Fahrni, *Chem. Mater.*, 2011, **23**, 483; (*d*) D. Maity and T. Govindaraju, *Inorg. Chem.*, 2011, **50**, 11282; (*e*) J. F. Jang, Y. Zhou, J. Yoon and J. S. Kim, *Chem. Soc. Rev.*, 2011, **40**, 3416; (*f*) P. Song, X. Chen, Y. Xiang, L. Huang, Z. Zhou, R. Wei and A. Tong, *J. Mater. Chem.*, 2011, **21**, 13470.

20 (*a*) S. Karupannan and J. C. Chambron, *Chem.–Asian. J*, 2011, **6**, 964 and references therein; (*b*) L. Fabbrizzi, M. Lichelli, P. Pallavicini, D. Sacci and E. Taglietti, *Analyst*, 1996, **121**, 1763.

21 (*a*) M. Kumar, R. Kumar and V. Bhalla, *Org. Lett.*, 2011, **13**, 366; (*b*) K. H. Chen, J. S. Yang, C. Y. Hwang and M. Feng, *Org. Lett.*, 2008, **10**, 4401; (*c*) L. Basabe-Desmonts, D. N. Reinhoudt and M. Crego-Calama, *Chem. Soc. Rev.*, 2007, **36**, 993; (*d*) J. M. Kim, S. J. Min, S. W. Lee, J. H. Bok and J. S. Kim, *Chem. Commun.*, 2005, 3427; (*e*) H. J. Kim, S. Bhuniya, R. K. Mahajan, R. Puri, H. Liu, K. C. Ko, J. Y. Lee and J. S. Kim, *Chem. Commun.*, 2009, 7128.

22 M. R. Silva-Junior and W. J. Thiel, *J. Chem. Theory Comput.*, 2010, **6**, 1546.

23 (*a*) I. Yildiz, M. Tomasulo and F. M. Raymo, *J. Mater. Chem.*, 2008, **18**, 5577; (*b*) B. Yoon, D. Y. Ham, O. Yarimaga, H. An, C. W. Lee and J. M. Kim, *Adv. Mater.*, 2011, **23**, 5492.

24 (*a*) S. Muthaiah, Y. C. Rajan and H. C. Lin, *J. Mater. Chem.*, 2012, **22**, 8976; (*b*) R. Satapathy, Y. S. Wu and H. C. Lin,

Published on 05 November 2012. Downloaded by National Chiao Tung University on 28/04/2014 02:09:41.

Chem. Commun., 2012, **48**, 5668; (*c*) R. Satapathy, Y. S. Wu and H. C. Lin, *Org. Lett.*, 2012, **14**, 2564; (*d*) R. Satapathy, H. Padhy, Y. H. Wu and H. C. Lin, *Chem.–Eur. J.*, 2012, DOI: 10.1002/chem.201201437.

25 W. Zhou, Y. Li, Y. Li, H. Liu, S. Wang, C. Li, M. Yuan, X. Liu and D. Zhu, *Chem.–Asian. J.*, 2006, **1–2**, 224–230.

26 (*a*) H. C. Chu, Y. H. Lee, S. J. Hsu, P. J. Yang, A. Yabushita and H. C. Lin, *J. Phys. Chem. B*, 2011, **115**, 8845; (*b*) P. J. Yang, H. C. Chu, T. C. Chen and H. C. Lin, *J. Mater. Chem.*, 2012, **22**, 12358.

27 J. Li, Y. Wu, F. Song, G. Wei, Y. Cheng and C. Zhu, *J. Mater. Chem.*, 2012, **22**, 478.

28 (*a*) G. Grynkiewcz, M. Poenie and R. Y. Tsein, *J. Biol. Chem.*, 1985, **260**, 3440; (*b*) M. H. Yang, P. Thirupathi and K. H. Lee, *Org. Lett.*, 2011, **13**, 5028; (*c*) D. Maity and T. Govindaraju, *Chem. Commun.*, 2012, **48**, 1039.

29 (*a*) K. Cammann, U. Lemke, A. Rohen, J. Sander, H. Wilken and B. Winter, *Angew. Chem., Int. Ed. Engl.*, 1991, **30**, 516; (*b*) P. D. Beer and P. A. Gale, *Angew. Chem., Int. Ed.*, 2001, **40**, 486; (*c*) G. Zhang, D. Zhang, S. Yin, X. Yang, Z. Shuai and D. Zhu, *Chem. Commun.*, 2005, 2161; (*d*) B. Ma, F. Zeng, F. Zheng and S. Wu, *Chem.–Eur. J.*, 2011, **17**, 14844.

30 K. J. Albert, N. S. Lewis, C. L. Schauer, G. A. Sotzing, S. E. Stitzel, T. P. Vaid and D. R. Walt, *Chem. Rev.*, 2000, **100**, 2595.

31 (*a*) M. H. Ha-Thi, M. Penhoat, D. Drouin, M. Blanchard-Desce, V. Michelet and I. Leray, *Chem.–Eur. J.*, 2008, **14**, 5941; (*b*) M. Schaferling, *Angew. Chem., Int. Ed.*, 2012, **51**, 3532.

32 Y. Hong, J. W. Y. Lam and B. Z. Tang, *Chem. Commun.*, 2009, 4332.

33 (*a*) M. Cai, Z. Gao, X. Zhou, X. Wang, S. Chen, Y. Zhao, Y. Qian, N. Shi, B. Mi, L. Xie and W. Huang, *Phys. Chem. Chem. Phys.*, 2012, **14**, 5289; (*b*) Y. Hong, L. Meng, S. Chen, C. W. T. Leung, L. T. Da, M. Faisal, D. A. Silva, J. Liu, J. Wing, Y. Lam, X. Huang and B. Z. Tang, *J. Am. Chem. Soc.*, 2012, **134**, 1680; (*c*) A. Qina, J. W. Y. Lamb and B. Z. Tang, *Prog. Polym. Sci.*, 2012, **37**, 182.

 This journal is © The Royal Society of Chemistry 2013